Low power AlGaN/GaN MEMS pressure sensor for high vacuum application

Sun, Jianwen; Hu, Dong; Liu, Zewen; Middelburg, Luke M.; Vollebregt, Sten; Sarro, Pasqualina M.; Zhang, Guoqi

DOI
10.1016/j.sna.2020.112217

Publication date
2020

Document Version
Final published version

Published in
Sensors and Actuators, A: Physical

Sensors and Actuators A 314 (2020) 112217

Contents lists available at ScienceDirect

Sensors and Actuators A: Physical

journal homepage: www.elsevier.com/locate/sna

Low power AlGaN/GaN MEMS pressure sensor for high vacuum application

Jianwen Sun[a,b,1], Dong Hu[a,1], Zewen Liu[c], Luke M. Middelburg[a], Sten Vollebregt[a], Pasqualina M. Sarro[a,*], Guoqi Zhang[a,*]

[a] Department of Microelectronics, Delft University of Technology, 2628 CD, Delft, the Netherlands
[b] Shenzhen Institute of Wide-bandgap Semiconductor, 518071, Shenzhen, China
[c] Institute of Microelectronics, Tsinghua University, 100084, Beijing, China

ARTICLE INFO

Article history:
Received 2 March 2020
Received in revised form 7 June 2020
Accepted 19 July 2020
Available online 26 July 2020

Keywords:
AlGaN/GaN
MEMS
Pressure sensor
Vacuum

ABSTRACT

A micro-scale pressure sensor based on suspended AlGaN/GaN heterostructure is reported with non-linear sensitivity. By sealing the cavity, vacuum sensing at various temperatures was demonstrated. To validate the proposed concept of the AlGaN/GaN vacuum sensor, a 700 μm diameter circular membrane was electrically characterized under applied static and dynamic pressures at various temperatures ranging from 25 °C to 100 °C. The current change of the AlGaN/GaN heterostructure increased as the vacuum and temperature increases due to the increase of 2DEG density by tensile strain. The dynamic current change from 96 kPa down to 10 Pa of AlGaN/GaN heterostructure pressure sensor was 18.75 % at 100 °C. The maximum sensitivity reached 22.8 %/kPa with a power consumption of 1.8 μW. These results suggest that suspended AlGaN/GaN heterostructures are promising for high vacuum and high-temperature sensing applications.

1. Introduction

Recently, compact MEMS pressure detection gains more attention for several applications such as RF switches [1], energy harvesters [2,3] and MEMS resonators [4]. These systems, while contain moving parts, have to maintain a vacuum environment ($1 \times 10^{-5} \sim 10^{-3}$ Torr) for proper operation. Besides MEMS devices, advanced scientific instruments, such as electron microscopes and ion mass spectrometers, require a high vacuum environment. Therefore, it is desirable to monitor the vacuum pressure and minimize the size of pressure gauges. Most vacuum sensors or gauges can be classified into three types: ionization vacuum, thermal conductivity and mechanical. Ionization vacuum gauges have been commercially used to detect high vacuum, but the efficient electron and a sufficient electron path requirements impede miniaturization. Thermal conductivity gauges have a simple structure and are therefore suitable for miniaturization, such as a Pirani gauge. However, this is undesired because such a gauge cannot be universily applied among varying gas compositions. Another type of vacuum sensor is mechanical gauges, such as cantilevers and membranes, which deform with the change of pressure. The representative mechanical gauges are based on the membrane structure [5]. The membrane deforms due to the pressure difference from both sides, causing an electronic change of capacitance or resistance [6]. However, the conventional Si-based membrane is likely to suffer failure from material fatigue by long-term loading and high-temperature environment [7,8].

AlGaN/GaN heterostructures attract extensive attention because of the high sheet density of two-dimensional electron gas (2DEG) introduced by the large piezoelectric and spontaneous polarization charges [9,10]. Lots of research has been done focusing on microwave [11] and power [12] devices thanks to the robust performance in high temperature or high radiation environment. Additionally, thanks to the wide bandgap semiconductor properties, AlGaN/GaN heterostructure based sensors have been reported for various sensing applications such as pressure [13–16], gases [17–19] and optical [20–22]. Compared to silicon carbide (SiC), the piezoresistive gauge factor of AlGaN/GaN heterostructures is approximately three times higher than the highest gauge factor reported for SiC [23], which represents the potential of AlGaN/GaN heterostructures in high-temperature pressure sensing applications. Such a device can be realized by etching away the substrate to form a MEMS structure and building the AlGaN/GaN sensing

* Corresponding authors.
E-mail addresses: P.M.Sarro@tudelft.nl (P.M. Sarro), G.Q.Zhang@tudelft.nl (G. Zhang).
[1] These authors are contributed equally to this work.

https://doi.org/10.1016/j.sna.2020.112217
0924-4247/

element on it. The sensitivity in the field of pressure sensors is usually considered as the change of capacitance [24], output current [25,26] or voltage [27] of the device with applied pressure, which could be enhanced by lowering the gate bias of the transistor [14,28] or increasing the Al content of the AlGaN layer [14]. It can be concluded from literature that most of the prior works on AlGaN devices are only capable of measuring over-pressures instead of vacuum (thus pressures exceeding 100 kPa (absolute)). Therefore, the goal of this paper is to develop a micro fabricated AlGaN/GaN MEMS pressure sensor with maximized local sensitivity in the vacuum regime. Any induced non-linearity in the response of the sensor will be investigated. Furthermore, the effect of both pressure and temperature on the drain current of an AlGaN/GaN heterostructure will be investigated while taking into account the dynamic and static performace of the devices at various temperatures.

2. Experiments

The AlGaN/GaN structure consists of an undoped Ga-face GaN buffer layer (2 μm), followed by an AlN interlayer (1 nm), an undoped $Al_{0.26}Ga_{0.74}N$ barrier layer (25 nm), and a 3 nm GaN cap layer as shown in Fig. 1(a). The epilayers were grown on a 1 mm thick <111> silicon wafer using metal-organic chemical vapor deposition (MOCVD). The fabrication process started with a mesa etch to define the active area. Then, Ti/Al/Ti/Au ohmic metallization was deposited by e-beam evaporation and patterned by lift-off and annealed at 870 °C for 45 s under N_2 ambient. Next, an evaporated Ti/Pt layer was patterned by lift-off to form the microheater, followed by a 200-nm plasma-enhanced chemical vapor deposition (PECVD) SiO_2 layer to isolate the heater from the interconnect layer. The evaporated Ti/Au layer stack is then used to form the metal interconnect. The topside of the wafer was passivated with a 300 nm PECVD SiO_2 layer and the backside was thinned down to 400 μm by chemical mechanical polishing (CMP). The SiO_2 layer on the top side of the wafer was etched in a buffered oxide etch (BOE) solution to open the contact pads and gate windows. The silicon substrate was etched from the backside by deep reactive ion etching (DRIE) using a 5 μm-thick SiO_2 layer as the hard mask to form a circular membrane (700 μm in diameter). After dicing, the sensor was bonded to a second silicon wafer using silicone (BISON) to create a reference pressure (101 kPa) as shown in Fig. 1(a) and (b). The thickness of the GaN membrane was about 5 μm as illustrated in Fig. 1(c). Then the sensor was put in a pressure chamber integrated with a temperature-controllable microprobe station (NEXTRON) and electrically connected to a Keithley 2612B source measure unit (SMU).

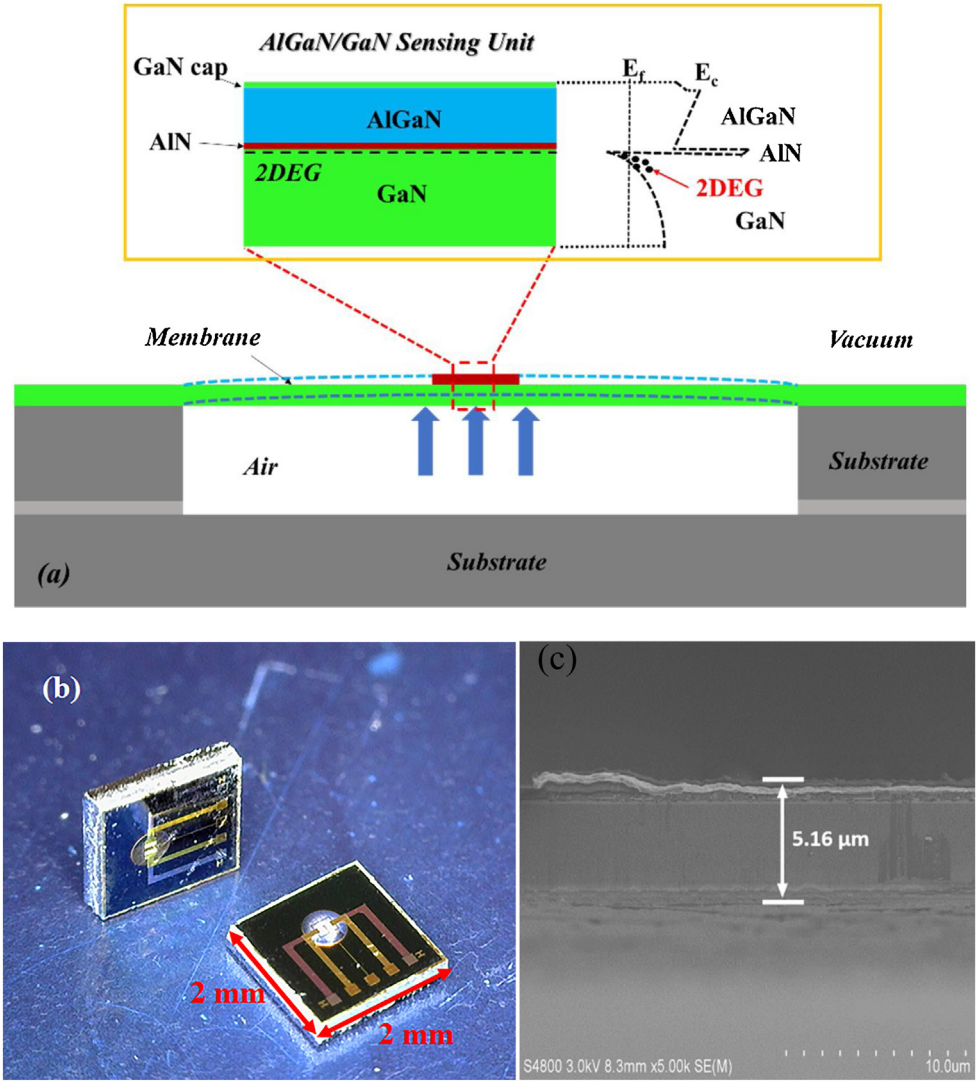

Fig. 1. (a) A schematic image of MEMS AlGaN/GaN pressure sensor; (b) An optical image of a micro-fabricated AlGaN/GaN heterostructure sensor; (c) An SEM image of the GaN membrane cross-section.

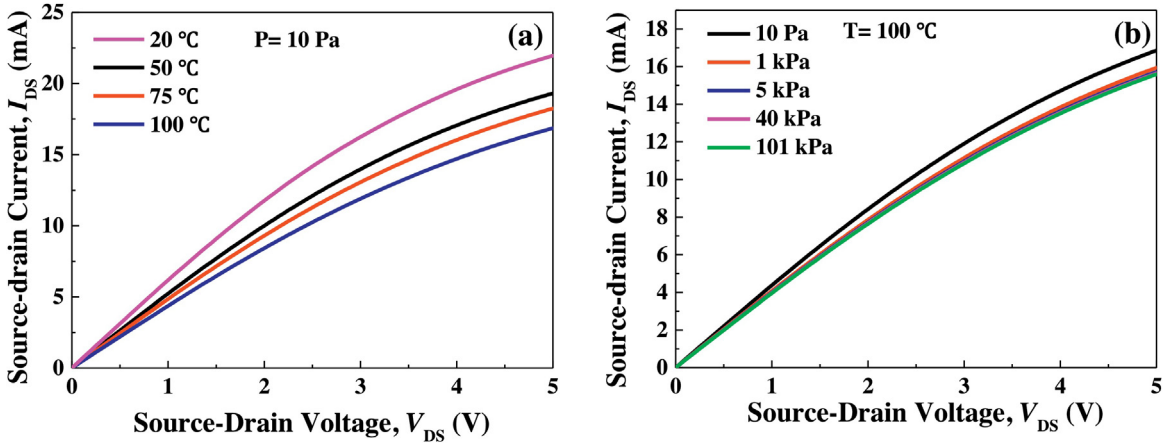

Fig. 2. I-V static response of MEMS AlGaN/GaN pressure sensor versus temperature (a) and pressure (b).

The temperature was controlled by the microprobe station used and the integrated microheater was used to modulate the membrane temperature to improve sensitivity. More details about the process of GaN-based sensors can be found in earlier publications [17,20,29].

3. Results and discussion

3.1. Static measurement

The I_{DS}-V_{DS} static response of the AlGaN/GaN heterostructure pressure sensor at various temperature and pressure values is shown in Fig. 2. From Fig. 2(a), it can be seen that the drain current decreases with the increasing temperature at ~ 10 Pa, which is attributed to a large decrease in channel mobility [30] and piezoelectric effect [31] of the HEMT device. Furthermore, the drain current of the device increases with increasing pressure, as reported in Fig. 2(b), which is attributed to an increase of 2DEG density (N_S) by the enhanced piezoelectric polarization [13,31–33]. However, it can be found that the sensor current change versus vacuum pressure in the range from 101 kPa to 1 kPa was much smaller than that from 1 kPa to 10 Pa, which is caused by the smaller deflection at the vacuum pressure range from 101 kPa to 1 kPa. Therefore, this sensor shows better performance in the lower pressure range. The static current change ($\Delta I_{DS}/I_{DS,101\,kPa}$, where ΔI_{DS} is the relative change in drain current under the loading pressure, $I_{DS,101\,kPa}$ is the reference drain current at atmospheric pressure) [31,34] of the AlGaN/GaN heterostructure sensor is shown in Fig. 3 as a function of source-drain voltage (V_{DS}) at various temperatures and vacuum pressure values. From Fig. 3(a), a larger percent current change can be found at a higher temperature, which is caused by the thermal-induced deflection of the membrane at higher temperatures [35]. Consequently, the larger deflection introduced more tensile strain in the device, which led to an increase in piezoelectric polarization and then increases the 2DEG density and I_{DS} [13,14,31–33]. This could also explain the observed increase in I_{DS} with decreasing pressure values as shown in Fig. 3(b). Moreover, at a constant temperature, the percent current change of the AlGaN/GaN sensor slightly decreases with increasing V_{DS}. This phenomenon might be caused by the self-heating effect, which results in the elevated channel temperature [28].

3.2. Dynamic measurement

In order to examine the dynamic characterization of the device, the pressure firstly was increased from 10 Pa to 96 kPa and then swept back to 10 Pa. The pressure was maintained for 300 s at each pressure set point. In Fig. 4(a), keeping V_{DS} = 20 mV and T = 100 °C, the measured pressure profile and the drain current of sensor versus pressure are indicated by the blue and red curves respectively. The output curve showed a recoverable response to the pressure change and the working power consumption of the device was about 1.8 μW. It can be seen that the drain current decreases when a lower vacuum environment is applied, and that the overall current change equals 18.75 %. Furthermore, as shown in Fig. 4(b), a repeatable response of the drain current was observed when the pressure was swept back and forth from 600 Pa to 5 kPa for 5 cycles at various temperatures. The current response follows the change of pressure immediately as shown in Fig. 4(c). In addition, the percent current change increases with the temperature when the vacuum pressure changes from 5 kPa to 600 Pa as shown in Fig. 4 (d), which supports the AlGaN/GaN sensor to have a large response at a higher temperature. The dynamic percent drain current change of sensor at various temperatures is shown in Fig. 5. Temperatures beyond 50 °C and ambient pressures below 5 kPa result in current change increasing, especially at a pressure below 1 kPa, a significant increase in current change is observed as shown in the inset, indicating a higher sensitivity in low pressure range. At 100 °C, the sensitivity varied from 0.005 %/kPa (70 kPa – 40 kPa) to 22.8 %/kPa (600 Pa – 10 Pa). Compared with prior similar works on AlGaN/GaN pressure sensors, as shown in Table 1, the ability of vacuum sensing was tested instead of using the sensor at over-pressure beyond atmospheric. Another difference is that the sensing voltage used in this work is much lower than other AlGaN/GaN HEMT pressure sensor reported in literature. In addition, our study applied dynamic pressure profiles, which enables the investigation of dynamic behavior and repeatability. Although Durga et al. [24] applied dynamic differential pressure, more pressure stages were adopted in this work. Most importantly, our work presented a non-linear sensitivity to the vacuum level. Especially in the low pressure range below 600 Pa, the maximum sensitivity is significantly larger than other works as 22.8 % at 100 °C. This result suggests the feasibility of the AlGaN/GaN sensor for the applications in high-vacuum and high-temperature.

3.3. Working principle of pressure sensing

In order to further understand the working mechanism of the vacuum pressure sensor, the energy band diagram of the AlGaN/GaN heterostructure under tension condition is illustrated in Fig. 6. Under strain-free conditions, the 2DEG is formed in the GaN surface close to the AlGaN/GaN interface because of the large piezoelectric and spontaneous polarization charges. The 2DEG

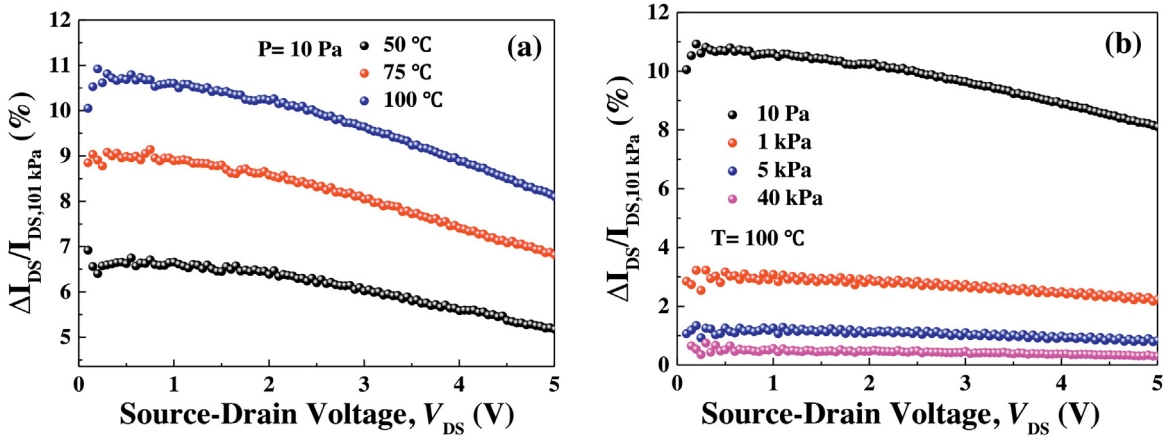

Fig. 3. Static percent current change of the AlGaN/GaN sensor as a function of source-drain voltage versus temperature (a) and vacuum pressure (b).

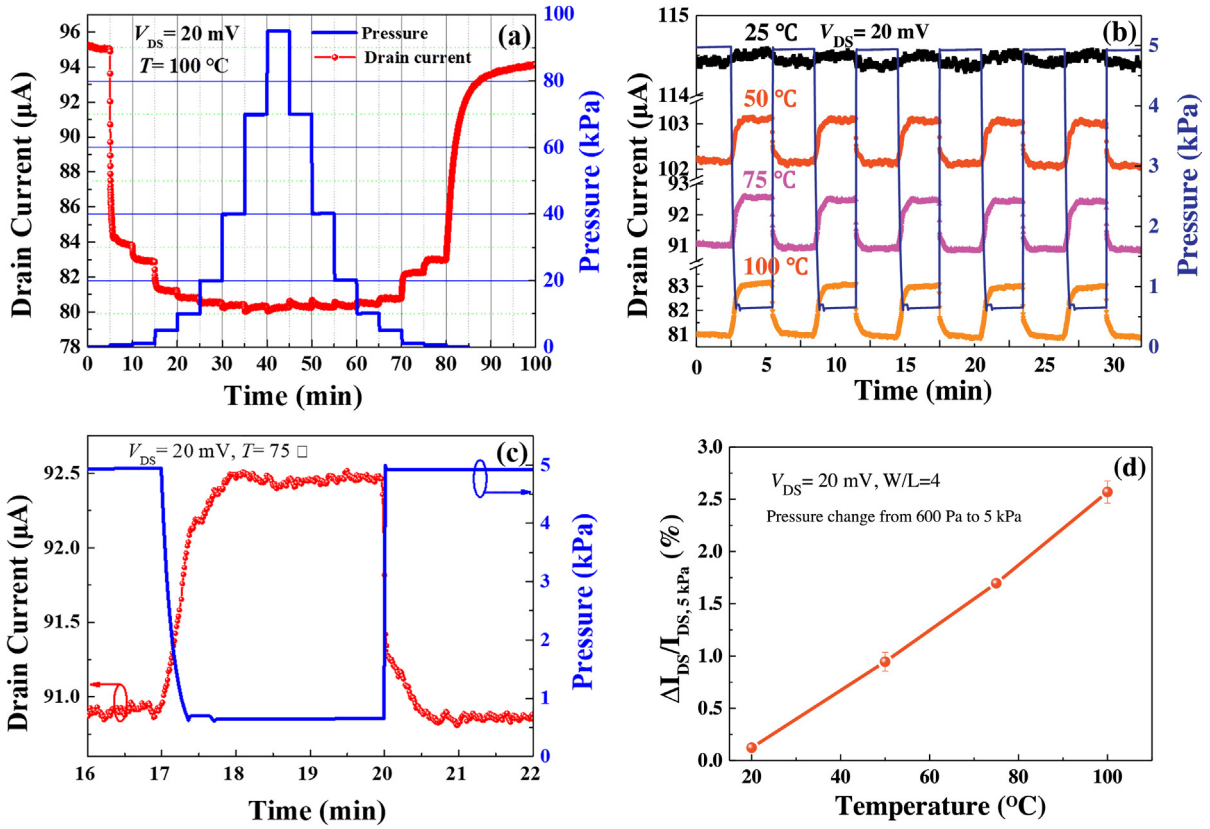

Fig. 4. (a) The output drain current (red curve) of AlGaN/GaN sensor as a function of pressure at V_{DS} = 20 mV and T=100 °C (the blue curve shows the set pressure profile) and; (b) Sensing repeatability of the device at various temperatures when pressure is swept from 600 Pa to 5 kPa; (c) Drain current response follows the change of the pressure during one cycle; (d) Percent current change (from 600 Pa to 10 Pa) versus the temperature (For interpretation of the references to colour in this figure legend, the reader is referred to the web version of this article).

Table 1
Comparison of the fabricated sensor and prior works on GaN-based pressure sensors.

	Our work	Durga et al. [24]	Xin et al. [36]	Caitlin et al. [14]	Nam-In et al. [37]
Materials	AlGaN/GaN	AlGaN/GaN	AlGaN/GaN	InAlN/GaN	GaN
Max. sensitivity	22.8 %/kPa (Non-linear)	0.76 %/kPa	72 μV/kPa/V (Linear)	0.09 %/kPa (0.64 %/psig Linear)	0.17 %/kPa (1.26 %/psig Linear)
V_{DS}	0.02 V	1.5 V	1–5 V	0 – 8 V	/
Temperature	25 – 100 °C	25 – 200 °C	25 °C	25, 300 °C	25 – 400 °C
Pressure range	0.01 – 96 kPa	101, 131 kPa	101 – 1000 kPa	101 – 297kPa	345 – 1379 kPa

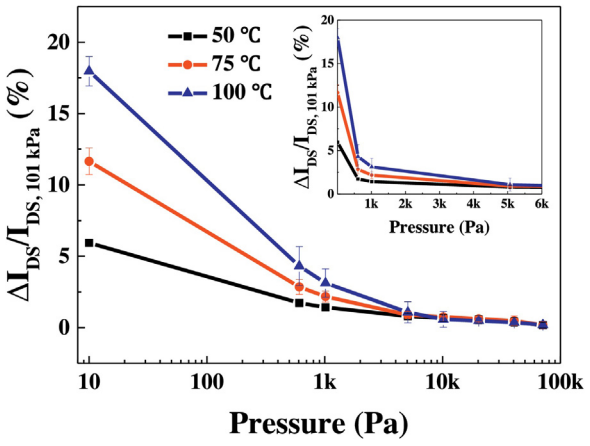

Fig. 5. Dynamic percent current change of the device versus pressure at various temperatures.(The inset is the current change versus pressure in linear scale of 0-6 kPa).

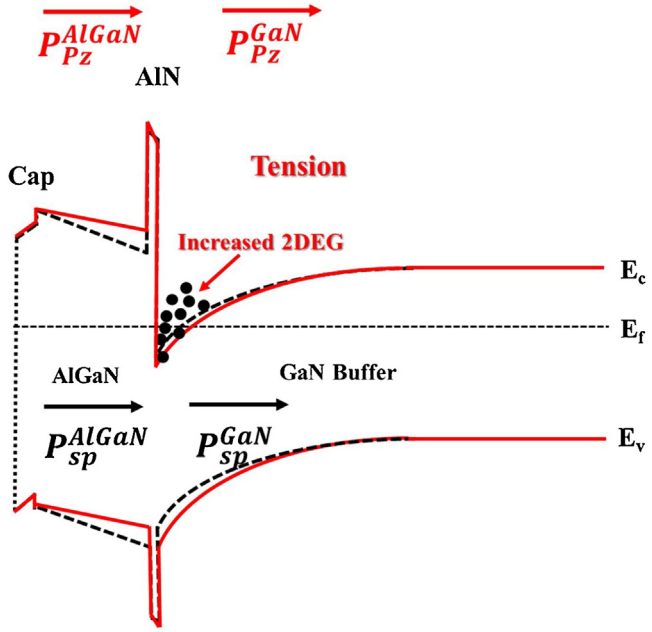

Fig. 6. Energy band diagram of AlGaN/GaN heterostructure pressure under tension condition. (E_c: conduction band; E_f: Fermi level; E_V: valence band).

density (N_S) and sheet charge density (σ_{Pol}) at the AlGaN/GaN heterostructure interface is given by [32]

$$N_s = \frac{\sigma_{Pol}}{e} - \left(\frac{\varepsilon_0 \varepsilon}{d_d e^2}\right)(e\phi_B + E_F - \Delta E_C) \quad (1)$$

$$\sigma_{Pol} = P_{AlGaN(Sp)} + P_{AlGaN(Pz)} - P_{GaN(Sp)} - P_{GaN(Pz)} \quad (2)$$

Where e is the elementary charge, ε_0 is the electric permittivity, ε is the relative permittivity of AlGaN, d_d is the AlGaN layer thickness, $e\phi_B$ is the barrier height of the gate contact on AlGaN, E_F is the Fermi level, ΔE_C is the conduction band offset. The spontaneous polarization of $Al_{0.26}Ga_{0.74}N$ [$P_{AlGaN\ (Sp)}$] and GaN [$P_{GaN\ (Sp)}$] are -0.042 C/m^2 and -0.029 C/m^2, respectively [32]. Under a strain-free condition, the piezoelectric polarization of GaN [$P_{GaN\ (Pz)}$] is equal to zero [38]. The $P_{AlGaN\ (Pz)}$ is the piezoelectric polarization of AlGaN that is induced by the lattice mismatch strain follows [39]

$$P_{AlGaN(Pz)} = 2[1 - r(x)] \times \frac{a_{GaN} - a_{AlGaN}}{a_{AlGaN}}\left(e_{31} - e_{33}\frac{c_{13}}{c_{33}}\right) \quad (3)$$

Where, $r(x) = \frac{a_{AlGaN,strained} - a_{GaN}}{a_{AlGaN,relaxed} - a_{GaN}}$, $a_{AlGaN,strained}$ and $a_{AlGaN,relaxed}$ are the lattice constant of AlGaN barrier under stress and relaxed conditions respectively, e_{33} and e_{31} are the piezoelectric coefficients of the AlGaN barrier layer, c_{13} and c_{33} are the elastic constants of the $Al_xGa_{1-x}N$ barrier layer, a_{GaN} and a_{AlGaN} are the lattice constant of the GaN layer and relaxed AlGaN layer respectively. The value of $\left(e_{31} - e_{33}\frac{c_{13}}{c_{33}}\right)$ is always negative, therefore under tensile strain ($a_{GaN} > a_{AlGaN}$) the magnitude of piezoelectric polarization is negative and for compressive strain ($a_{GaN} < a_{AlGaN}$), it is positive. Since the spontaneous polarization is always negative and points towards the substrate (in Ga-face) for GaN and AlGaN as shown in Fig. 6, the alignment of spontaneous and piezoelectric polarization is parallel for tensile stain and anti-parallel for compressive strain. Therefore, under tension conditions, the negative piezoelectric polarization charges are introduced along with the AlGaN/GaN interface and the energy band of AlGaN close to AlGaN/AlN interface tilts upward and the energy band of GaN near AlN/GaN interface is bent down. Meanwhile, the increased sheet charge density (σ_{Pol}) results in more free electrons and the 2DEG increasing. In addition, the 2DEG mobility μ is dependent on the collision time (τ_c) and the effective mass (m_{eff}) of the 2DEG electron. The temperature predominantly changes the collision time (τ_c) and the strain changes the effective mass (m_{eff}). The average effective mass is about 0.25 %/100 MPa under biaxial strain from [40], which could be negligible in this case. Ideally, the temperature dependence of the mobility is given by [41]

$$\mu_T = \mu_0\left(\frac{T}{300}\right)^{-\theta_T} \quad (4)$$

Where μ_0 is the mobility at 300 K and θ_T is the temperature coefficient of the mobility, $\theta_T = 1.5$ used in [41]. Thus, the 2DEG conductivity decreases with the temperature mainly due to the decrease in the 2DEG mobility. Meanwhile, the influence of temperature on 2DEG density is neglected compared to the change in electron mobility [42]. Therefore, the base drain current (I_{Base}) decreases as temperature increases under atmospheric pressure, which is consistent with the experimental results in Fig. 2(a). Because the cavity is sealed, the pressure in the cavity (P_{IN}) will increase with increasing temperature. This pressure can be described by the ideal gas law, while taking into account the limited volume:

$$PV = nRT$$

In which V the volume, n is the amount of substance, R the ideal gas constant and T the absolute temperature in Kelvin.

If the vacuum pressure (P_{Out}) in the testing chamber is kept constant, the difference pressure ($\Delta P = P_{In} - P_{Out}$) between the inside pressure and the outside pressure increases with increasing temperature. As a result the tensile strain increases and enhanced piezoelectric polarization is achieved, which results in an increase of 2DEG density. This suggests that an increase in the drain current change with increasing temperature at the same P_{Out}. It is noticeable that the temperature effect on the drain current change would be more evident in low pressure range (P_{Out} < 1 kPa). For instance, P_{In} would increase from 101 kPa to 126 kPa when the temperature changes from 25 °C to 100 °C and this pressure change is significantly larger than P_{Out}, resulting in a rapid increase in the drain current change and sensitivity. The sensor sensitivity S of AlGaN/GaN heterostructure pressure sensor increases with the temperature given by the following equation:

$$S\uparrow = \left(\frac{\Delta I\uparrow}{I_{Base}\downarrow}\right)_{T\uparrow} = \left(\frac{I_P\uparrow - I_{Base}\downarrow}{I_{Base}\downarrow}\right)_{T\uparrow} \quad (5)$$

Where I_{Base} and I_P are the drain current of device at ambient air and target pressure conditions. ΔI is the current change introduced by the change of pressure. Based on the measurement results, it can be

concluded if the temperature T increases, I_{Base} will decrease and I_P will increase. Therefore, the sensor response would increase with the temperature under a constant pressure.

4. Conclusion

In conclusion, a suspended membrane AlGaN/GaN heterostructure sensor showed a rapid response in drain current change when exposed to different pressures, especially in the low-pressure range below 600 Pa. The dynamic percent current change of the AlGaN/GaN heterostructure pressure sensor was 18.75 % when pressure changed from 96 kPa to 10 Pa at 100 °C with a low power consumption of 1.8 μW. The maximum sensitivity was obtained as 22.8 %/kPa with pressure ranging from 600 Pa to 10 Pa. Moreover, the basic mechanism of AlGaN/GaN heterostructure pressure sensing and temperature effect was discussed. Under the tension strain condition, the negative spontaneous polarization led to the increase of the 2DEG density, resulting in an increase of the drain current. In terms of the effect of temperature, thermal-induced deflection of the membrane also enhanced the increase of the 2DEG density. Therefore, the larger sensor response was detected at a higher temperature. All in all, both results of static and dynamic measurement demonstrate the potential of suspended MEMS AlGaN/GaN heterostructure pressure sensors for high vacuum and high-temperature applications.

CRediT authorship contribution statement

Jianwen Sun: Conceptualization, Resources, Writing - original draft. **Dong Hu:** Methodology, Investigation, Writing - review & editing. **Zewen Liu:** Supervision. **Luke M. Middelburg:** Resources, Writing - review & editing. **Sten Vollebregt:** Supervision, Resources. **Pasqualina M. Sarro:** Supervision, Writing - review & editing. **Guoqi Zhang:** Supervision, Project administration.

Declaration of Competing Interest

We declare that there are no conflicts of interest.

Acknowledgement

This research did not receive any specific grant from funding agencies in the public, commercial, or not-for-profit sectors. The authors acknowledge Dr. Henk van Zeijl of Else Kooi Laboratory for providing die-bonding solutions.

Appendix A. Supplementary data

Supplementary material related to this article can be found, in the online version, at doi:https://doi.org/10.1016/j.sna.2020.112217.

References

[1] Z. Gong, Y. Zhang, X. Guo, Z. Liu, Wafer-level packaging method for RF MEMS applications using pre-patterned BCB polymer, Micromachines 9 (3) (2018) 93.
[2] R. Elfrink, et al., Vacuum-packaged piezoelectric vibration energy harvesters: damping contributions and autonomy for a wireless sensor system, J. Micromechanics Microengineering 20 (10) (2010) 104001.
[3] R. Elfrink, et al., Vibration energy harvesting with aluminum nitride-based piezoelectric devices, J. Micromech. Microeng. 19 (9) (2009) 094005.
[4] G. Wu, D. Xu, B. Xiong, Y. Wang, Y. Wang, Y. Ma, Wafer-level vacuum packaging for MEMS resonators using glass frit bonding, J. Microelectromechanical Syst. 21 (6) (2012) 1484–1491.
[5] F. Völklein, A. Meier, Microstructured vacuum gauges and their future perspectives, Vacuum 82 (4) (2007) 420–430.
[6] A. Górecka-Drzazga, Miniature and MEMS-type vacuum sensors and pumps, Vacuum 83 (12) (2009) 1419–1426.
[7] J. Courbat, D. Briand, N.F. de Rooij, Reliability improvement of suspended platinum-based micro-heating elements, Sens. Actuators A Phys. 142 (1) (2008) 284–291.
[8] G. Korotcenkov, Porous Silicon: From Formation to Application: Biomedical and Sensor Applications, Volume Two, CRC Press, 2016.
[9] O. Ambacher, et al., Two dimensional electron gases induced by spontaneous and piezoelectric polarization in undoped and doped AlGaN/GaN heterostructures, J. Appl. Phys. 87 (1) (2000) 334–344.
[10] J.P. Ibbetson, P. Fini, K. Ness, S. DenBaars, J. Speck, U. Mishra, Polarization effects, surface states, and the source of electrons in AlGaN/GaN heterostructure field effect transistors, Appl. Phys. Lett. 77 (2) (2000) 250–252.
[11] Y. Hao, et al., High-performance microwave gate-recessed AlGaN/AlN/GaN MOS-HEMT with 73% power-added efficiency, Ieee Electron Device Lett. 32 (5) (2011) 626–628.
[12] J. Shi, L.F. Eastman, X. Xin, M. Pophristic, High performance AlGaN/GaN power switch with HfO 2 insulation, Appl. Phys. Lett. 95 (4) (2009) 042103.
[13] A. Wang, L. Zeng, W. Wang, Z. Luo, Static and dynamic simulation studies on the AlGaN/GaN pressure sensor, Semicond. Sci. Technol. 34 (11) (2019) 115022.
[14] C.A. Chapin, R.A. Miller, K.M. Dowling, R. Chen, D.G. Senesky, InAlN/GaN high electron mobility micro-pressure sensors for high-temperature environments, Sens. Actuators A Phys. 263 (2017) 216–223.
[15] J. Dzuba, et al., AlGaN/GaN diaphragm-based pressure sensor with direct high performance piezoelectric transduction mechanism, Appl. Phys. Lett. 107 (12) (2015).
[16] T. Lalinský, et al., Micromachined membrane structures for pressure sensors based on AlGaN/GaN circular HEMT sensing device, Microelectron. Eng. 98 (2012) 578–581.
[17] J. Sun, R. Sokolovskij, E. Iervolino, Z. Liu, P.M. Sarro, G. Zhang, Suspended AlGaN/GaN HEMT NO 2 gas sensor integrated with micro-heater, J. Microelectromechanical Syst. 28 (6) (2019) 997–1004.
[18] A. Bag, D.-B. Moon, K.-H. Park, C.-Y. Cho, N.-E. Lee, Room-temperature-operated fast and reversible vertical-heterostructure-diode gas sensor composed of reduced graphene oxide and AlGaN/GaN, Sens. Actuators B Chem. (2019) 126684.
[19] Y. Halfaya, et al., Investigation of the performance of HEMT-Based NO, NO(2) and NH(3) exhaust gas sensors for automotive antipollution systems, Sensors Basel (Basel) 16 (February (3)) (2016) 273.
[20] J. Sun, et al., Suspended tungsten trioxide (WO3) gate AlGaN/GaN heterostructure deep ultraviolet detectors with integrated micro-heater, Opt. Express 27 (25) (2019) 36405–36413, 2019/12/09.
[21] J. Sun, et al., Suppression of persistent photoconductivity AlGaN/GaN heterostructure photodetectors using pulsed heating, Appl. Phys. Express 12 (12) (2019) 122007.
[22] K.H. Lee, P.C. Chang, S.J. Chang, Y.C. Wang, C.L. Yu, S.L. Wu, AlGaN/GaN schottky barrier UV photodetectors with a GaN sandwich layer,(in english), IEEE Sens. J. 9 (July (7)) (2009) 814–819.
[23] M. Eickhoff, et al., Electronics and sensors based on pyroelectric AlGaN/GaN heterostructures–Part B: Sensor applications, Physica status Solidi (c) (6) (2003) 1908–1918.
[24] D. Gajula, I. Jahangir, G. Koley, High temperature AlGaN/GaN membrane based pressure sensors, Micromachines 9 (5) (2018) 207.
[25] C. Jiang, et al., Piezotronic effect tuned AlGaN/GaN high electron mobility transistor, Nanotechnology 28 (45) (2017) 455203.
[26] K. Yao, S. Khandelwal, F. Sammoura, A. Kazama, C. Hu, L. Lin, Piezoelectricity-induced Schottky barrier height variations in AlGaN/GaN high electron mobility transistors, Ieee Electron Device Lett. 36 (9) (2015) 902–904.
[27] T. Lalinský, et al., Piezoelectric response of AlGaN/GaN-based circular-HEMT structures, Microelectron. Eng. 88 (8) (2011) 2424–2426.
[28] E. Le Boulbar, et al., Effect of bias conditions on pressure sensors based on AlGaN/GaN High Electron mobility Transistor, Sens. Actuators A Phys. 194 (2013) 247–251.
[29] J. Sun, et al., Characterization of an acetone detector based on a suspended WO3-Gate AlGaN/GaN HEMT integrated with microheater, IEEE Trans. Electron Devices 66 (10) (2019) 4373–4379.
[30] A.S. Yalamarthy, D.G. Senesky, Strain-and temperature-induced effects in AlGaN/GaN high electron mobility transistors, Semicond. Sci. Technol. 31 (3) (2016) 035024.
[31] X. Wang, et al., Piezotronic effect modulated heterojunction electron gas in AlGaN/AlN/GaN heterostructure microwire, Adv. Mater. 28 (no. 33) (2016) 7234–7242.
[32] O. Ambacher, et al., Two-dimensional electron gases induced by spontaneous and piezoelectric polarization charges in N- and Ga-face AlGaN/GaN heterostructures, J. Appl. Phys. 85 (6) (1999) 3222–3233.
[33] A. Wang, L. Zeng, W. Wang, F. Calle, Modification of strain and 2DEG density induced by wafer bending of AlGaN/GaN heterostructure: influence of edges caused by processing, AIP Adv. 8 (3) (2018) 035318.
[34] Z. Lou, S. Chen, L. Wang, K. Jiang, G. Shen, An ultra-sensitive and rapid response speed graphene pressure sensors for electronic skin and health monitoring, Nano Energy 23 (2016) 7–14.
[35] J. Ren, M. Ward, P. Kinnell, R. Craddock, X. Wei, Plastic deformation of micromachined silicon diaphragms with a sealed cavity at high temperatures, Sensors 16 (2) (2016) 204.

[36] X. Tan, et al., High performance AlGaN/GaN pressure sensor with a Wheatstone bridge circuit„ Microelectron. Eng. 219 (2020) 111143.
[37] N.-I. Kim, et al., Piezoelectric pressure sensor based on flexible gallium nitride thin film for harsh-environment and high-temperature applications, Sens. Actuators A Phys. (2020) 111940.
[38] O. Ambacher, et al., Pyroelectric properties of Al (In) GaN/GaN hetero-and quantum well structures, J. Phys. Condens. Matter 14 (13) (2002) 3399.
[39] I.R. Gatabi, et al., PECVD silicon nitride passivation of AlGaN/GaN heterostructures, IEEE Trans. Electron Devices 60 (3) (2013) 1082–1087.
[40] M. Chu, A.D. Koehler, A. Gupta, T. Nishida, S.E. Thompson, Simulation of AlGaN/GaN high-electron-mobility transistor gauge factor based on two-dimensional electron gas density and electron mobility, J. Appl. Phys. 108 (10) (2010) 104502.
[41] S. Vitanov, V. Palankovski, S. Maroldt, R. Quay, High-temperature modeling of algan/gan hemts, Solid. Electron. 54 (10) (2010) 1105–1112.
[42] N. Maeda, K. Tsubaki, T. Saitoh, N. Kobayashi, High-temperature electron transport properties in AlGaN/GaN heterostructures, Appl. Phys. Lett. 79 (11) (2001) 1634–1636.

Biographies

Jianwen Sun received his M.S. degree in Microelectronics from Tsinghua University in 2015. He is currently pursuing the Ph.D degree in electrical engineering from Delft University of Technology, Delft, the Netherlands from 2015. His current research interests include design, fabrication and characterization of wide bandgap gallium nitride (GaN)-based UV and chemical sensors.

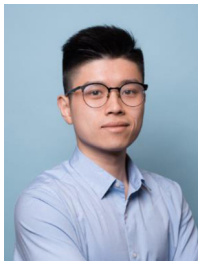

Dong Hu received his M.Sc degree in Nanotechnology from Kungliga Tekniska Högskolan (Sweden), and his B.Sc degree in Material Science and Engineering from Harbin Institute of Technology (China), in 2019 and 2016 respectively. From December 2019, he joined the Electronic Components, Technology and Materials (ECTM) group in Delft University of Technology, Delft, as a PhD researcher and works with Prof. Guoqi Zhang. His main research topic is nanomaterial-based advanced power electronics packages.

Zewen Liu received the B.S. degree in physics from the University of Science and Technology of China, Hefei, China, in 1983, and the Ph.D. degree in instrument physics from the University of Paris-Sud, Paris, France.,From 1983–1993, he was with Hefei National Synchrotron Radiation Laboratory. Since 1993, he has been with Tsinghua University, Beijing, China, where he is currently with the Institute of Microelectronics, and is engaged in novel IC devices and microsystem technologies.,Dr. Liu is a Senior Member of the Chinese Institute of Electronics and the Chinese Society of Micro/Nanotechnology.

Luke Middelburg was born in De Lier, The Netherlands, in 1993. He received the B.E. degree in Electrical Engineering in 2014 and the Master degree in Microelectronics in 2016, both at Delft University of Technology. In 2015 he joined the department of Electronic Instrumentation to work on the Ford Poling Challenge in the framework of the master thesis work. Currently he is working in the department of Electronic Components, Technology and Materials (ECTM) in the Else Kooi Laboratory, in the group of professor Kouchi Zhang. His main research topics are Wide Bandgap Semiconductor Sensors, harsh environment sensing and health monitoring.

Sten Vollebregt received his B.Sc. ('06) and M.Sc. ('09), both cum laude, in Electrical Engineering from Delft University of Technology. For his master thesis, he investigated the growth of carbon nanotubes at NanoLab, Newton, MA, USA and AIXTRON, Cambridge, UK. In 2014 he completed his Ph.D. thesis in the Microelectronics Department of the Delft University of Technology on the low-temperature high-density growth of carbon nanotubes for application as vertical interconnects in 3D monolithic integrated circuits. After obtaining his Ph.D., he held a post-doc position on the wafer-scale integration of graphene for sensing applications together with the faculty of Mechanical Engineering and several industrial partners. During this research, he developed a unique transfer-free wafer-scale CVD graphene process. Since Oct. 2017, he is an assistant professor in the Laboratory of Electronic Components, Technology and Materials of the Delft University of Technology where his research focuses on the integration of emerging electronic materials into semiconductor technology for sensing applications. His research interests are (carbon-based) nanomaterials, 3D monolithic integration, wide-bandgap semiconductors, and (harsh) environmental sensors. He has co-authored over 25 journal publications, 4 book chapters, and holds 3 patents.

Pasqualina M. Sarro (F'06) received the Laurea degree (cum laude) in solid-states physics from the University of Naples, Italy, in 1980, and the Ph.D. degree in electrical engineering from the Delft University of Technology, The Netherlands, in 1987. From 1981–1983, she was a Post-Doctoral Fellow with the Division of Engineering, Photovoltaic Research Group, Brown University, Rhode Island, USA. Since then, she has been with the Delft Institute of Microsystems and Nanoelectronics, Delft University of Technology, where she has been responsible for research on integrated silicon sensors and MEMS technology. In 2001, she became an A. van Leeuwenhoek Professor. Since 2004, she has been the Head of the Electronic Components, Materials, and Technology Laboratory. Since 2009, she has been the Chair of the Microelectronics Department, Delft University. She has authored or co-authored over 400 journals and conference papers. In 2006, she became a member of the Royal Netherlands Academy of Arts and Sciences. She is a member of the Technical Program Committee and the International Steering Committee for several international conferences, including the IEEE MEMS, the IEEE Sensors, Eurosensors, and Transducers. In 2006, she was elected as an IEEE Fellow for her contribution to micromachined sensors, actuators, and microsystems. In 2004, she received the EUROSENSORS Fellow Award for her contribution to the field of sensor technology. She is also the Technical Program Co-Chair of the First IEEE Sensors 2002 Conference and the Technical Program Chair of the Second and Third IEEE Sensors Conference in 2003 and 2004 and the General Co-Chair of the IEEE MEMS 2009. And she will act as General co-chair for IEEE Sensors 2014 and European TPC Chair for Transducers 2015.

Guo-Qi Zhang received the Ph.D. degree in aerospace engineering from the Delft University of Technology, Delft, The Netherlands, in 1993. He was with Philips for 20 years as Principal Scientist, from 1994 to 1996, the Technology Domain Manager, from 1996 to 2005, a Senior Director of Technology Strategy, from 2005 to 2009, and a Philips Fellow, from 2009 to 2013. He also had part time appointments as a Professor with the Technical University of Eindhoven, from 2002 to 2005, and the Chair Professor with the Delft University of Technology, from 2005 to 2013, where he has been the Chair Professor with the Department of Microelectronics, since 2013. As one of the renowned players in the fields of semiconductors and SSL technologies, he is also the Deputy Director of the European Center for Micro- and Nanoreliability (EUCEMAN), the Vice Chairman of the Chinese Electronics Packaging Association, and the China Co-Chairman of the Advisory Board of International Solid State Lighting Alliance (ISA). His current research interests include micro/nanoelectronics system integration, microsystems packaging, and assembly technologies and reliability.